RSC Advances

ROYAL SOCIETY OF CHEMISTRY

www.rsc.org/advances

Surface Initiated Polymerization of A-A/B-B Type Conjugated Monomers by Palladium Catalyzed Stille Polycondensation: Towards Low Band-Gap Polymer Brushes

Hussein Awada, Antoine Bousquet, Christine Dagron-Lartigau, Laurent Billon**

IPREM CNRS-UMR 5254, Equipe de Physique et Chimie des Polymères, Université de Pau et des Pays de l'Adour, Hélioparc, 2 avenue Président Angot, 64053 Pau Cedex 9, France

KEYWORDS low band gap polymer • hybrid nanoparticles • surface initiation • grafting • Stille polycondensation

ABSTRACT: Surface initiated polycondensation enables access to well-defined core-shell nanoparticles is described. Stille polymerization was initiated from the surface of palladium catalyst-immobilized zinc oxide nanorods. For the first time, a low band gap polymer poly[(4,4'-bis(2-ethylhexyl)dithieno-[3,2-b:2',3'-d]silole)-2,6-diyl-alt-(2,1,3-benzothiadiazole)-4,7-diyl] (PSBTBT) was anchored on zinc oxide nanorods to elaborate hybrid materials with tunable photophysical properties.

Ever since it was discovered that strong and flexible films of polyacetylene could be prepared by a Ziegler–Natta polymerization, numerous conjugated polymers have been synthesized for various applications: light-emitting diodes, sensors or photovoltaics.[1] The promises of organic-based devices are low cost, lightweight, conformability, flexibility and versatility due to the wide potential of chemical structures. At first, the concerns in the conjugated polymer chemistry field were to conceive new materials with improved control of electrical and optical properties and improved processibility; in particular to synthesize soluble conjugated polymers (CPs). A recent breakthrough in this field was the use of the so-called "low band gap" (LBG) polymers, able to harvest more photons than the "classical" such as CPs, poly(3-hexylthiophene) (P3HT).[2] These are often copolymers with alternated electron rich (donor) and electron deficient (acceptor) monomer units in their microstructure. The high energy level for the HOMO of the donor unit and the low energy level for the LUMO of the acceptor unit decrease the band gap due to an intra-chain charge transfer. Since the band gap of these polymers is lower than 1.8 eV, photons of wavelengths above 600 nm are absorbed. Thus photovoltaic efficiencies up to 10.8 % have been reached with these new macromolecules in bulk heterojunction with fullerene derivatives.[3-6]

In parallel, few research groups turned recently their attention toward the possibility to link conjugated polymers to inorganic, metal or carbon-based surfaces, by covalently binding the two components in order to design new hybrid materials.[7] Kiriy's and Locklin's research groups developed the so-called "surface initiated Kumada catalyst transfer polycondensation" (SI-KCTP) to create P3HT brushes from different substrates such as silica particles (core@shell, SiO2@P3HT), silicon, indium tin oxide or gold wafers.[8-11] Luscombe and colleagues developed SI-KCTP for the polymerization of 3-methylthiophene from an ITO wafer functionalized with an aryl-nickel-bromide initiator.[12] Very recently Bielawski's group extended the scope of surface initiated polymerization of conjugated monomer by performing the polycondensation of a phenylene-ethynilene A-B type monomer in a chain-growth manner.[13] Another methodology, called "grafting through" is based on the anchoring of a polymerizable group (most of the time a monomer) on the substrate. Polymer chain initiation takes place in solution or in bulk and during the propagation step; the growing chains react with the functional group attached to the surface and then further propagate with free monomers. This methodology has been applied for the grafting of conjugated macromolecules such as polyfluorene on quartz wafer via Yamamoto coupling polymerization [14] or poly(phenylene vinylene) on CdSe quantum dots via Heck coupling polycondensation [15].

For the moment, only a few conjugated macromolecules have been initiated from a surface and many synthetic efforts are still needed to find ways to covalently anchor CPs to a wide variety of surfaces (metal, metal oxide, etc). In this communication, we combine two very promising fields by reporting the elaboration of low band gap polymer brushes. The surface initiation of an (AA/BB) type step growth polymerization has been performed and zinc oxide@LBG nanoparticles were elaborated, for the first time.

In this report, poly[(4,4'-bis(2-ethylhexyl)dithieno-[3,2-b:2',3'-d]silole)-2,6-diyl-alt-(2,1,3-benzothiadiazole)-4,7-diyl] (PSBTBT) was synthesized from the polymerization of 4,7-dibromo-2,1,3-benzothiadiazole (M1) and 4,4'-bis(2-ethyl-hexyl)-5,5'-bis(trimethyltin)-dithieno[3,2-b:2',3'-d]silole (M2). This polymer was chosen for its broad absorption, high hole mobility, good photochemical stability and high power conversion efficiency of 5.1 %.[16] Monomers were obtained with high purity (97 % for M1 and 99 % for M2, synthesis and characterization in the Supporting Information, SI). They were first copolymerized in a chlorobenzene solution using Stille polycondensation. ^{1}H and ^{13}C Nuclear Magnetic Resonance (^{1}H/^{13}C NMR) showed all the characteristic peaks of the polymer and UV-visible spectrometry was used to evaluate the optical band gap as 1.52 eV (estimated from the low energy band edge of the optical spectrum, $Eg = 1240/\lambda onset$, Figure SI4). Although molar mass could not be measured by gel permeation chromatography (polymers insoluble in THF), comparison of the absorption spectra with literature confirmed that the degree of polymerization is high enough to reach the maximum conjugation length.[17]

Once the experimental conditions were successful for solution polymerization, they were transferred to surface initiated polymerization by functionalizing ZnO nanorods (length = 150 nm, ø = 30 nm and specific surface area = 24 $m^2.g^{-1}$) with initiating sites at the surface (Scheme 1). For this purpose a [2-((4-bromo-phenyl)-ethyl]-triethoxysilane (Si-PhBr) was synthesized (see SI) and grafted onto ZnO nanorods. In a second step the palladium catalyst ($Pd_2(dba)_3$, tris(dibenzylideneacetone)dipalladium(0)) was anchored to the substrate by creation of a phenyl-$Pd(dBa)_2$-Br complex. After each step, treated particles were purified from unreacted Si-PhBr or $Pd(dBa)_2$ and byproducts by repeated dispersion/centrifugation cycles. ZnO nanoparticles were chosen for their quality as electron acceptors making them of great use in hybrid solar cells. [12] Part of the reason for the low efficiency of hybrid photovoltaics [18] is related to properties of the ZnO/polymer interface. Because excitons formed in a polymer layer need to dissociate at the interface, contaminants that might exist at this interface will be very harmful. Therefore it is essential for an electron donor and an electron acceptor to be placed in direct contact for efficient dissociation of excitons.[19]

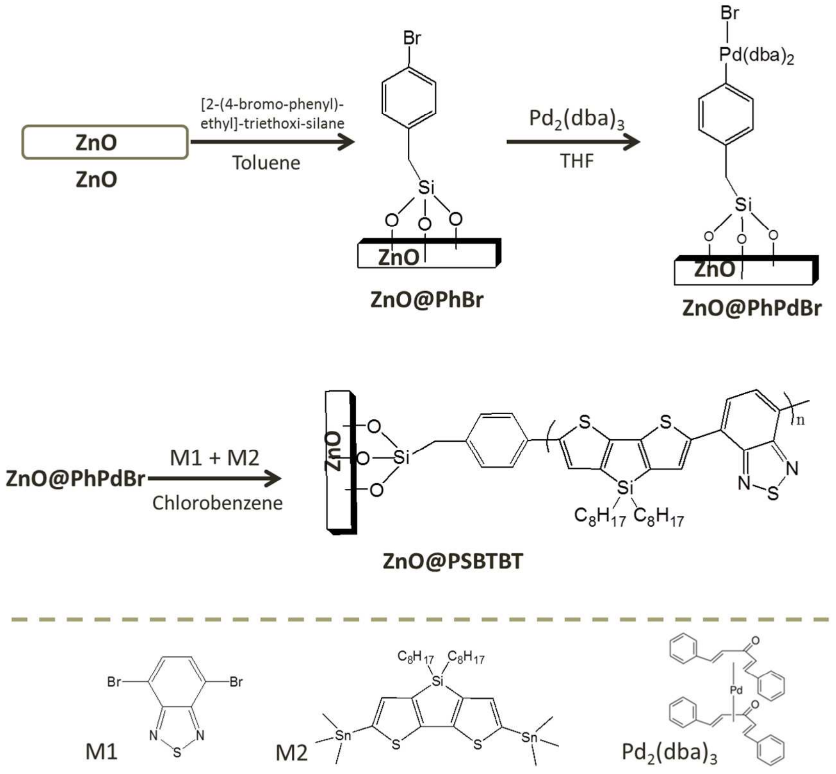

Scheme 1. Synthetic methodology of grafting low band gap polymer to zinc oxide particles.

The success of this grafting procedure was proven by X-ray photoelectron spectroscopy (XPS); Table 1 gives an overview of the surface chemical composition. When ZnO nanorods were functionalized with Si-PhBr, the zinc surface content decreased, the carbon one increased, and finally bromine and silicon appeared. From a quantitative point of view, thermogravimetric analysis (TGA) (Figure SI8) of ZnO and ZnO@PhBr showed an organic mass loss of 1.5 % which corresponded to a phenylbromide grafting density of 2 molecules.nm^{-2}. The aforementioned value was consistent with literature reports.[13, 20] Having proved the bromobenzene surface coverage of the ZnO nanorods, subsequent efforts were directed towards the anchoring of the palladium catalyst on the substrate. ZnO@PhBr nanorods were then reacted with an excess of $Pd_2(dba)_3$ (calculated from the specific surface area and the grafting density) in tetrahydrofurane (THF) at 50 °C for 6 h. The particles color turned from white to dark grey. XPS analysis of ZnO@PhPdBr showed a slight increase in the carbon content due to the dba ligands and the apparition of a peak at 335 eV pertaining to the palladium (Pd) element.

The surface polymerization was then performed from these ZnO@PhPdBr nanorods in a chlorobenzene solution of monomers M1 and M2 at 150 °C for 2, 4 and 6 h to obtain the particles ZnO@PSBTBT 2, 4 and 6, respectively. During the reaction, the dark brown solution turned first to dark blue and then to greenish, which is a clear sign of polymerization leading to conjugation length extension. The particles were then submitted to dispersion/centrifugation cycles several times, until the supernatant became colorless and its UV-visible spectrum was featureless. By this procedure, a consistent amount of “free” polymer (named PSBTBT 2, 4 and 6, respectively) was extracted from the core@shell particles. The fact that polymerization happened also in solution is inherent to the reaction process. In the present case, the polymerization was initiated from the particles since the catalyst was attached to their surface. Once a stannane monomer M2 reacts with ZnO@PhPdBr, the palladium catalyst is released from the surface to the solution and polymerization starts by activation of the brominated monomer M1. This polymerization being a step-growth reaction, the solution macromolecules may also couple to the substrate organic sites. The ratio between the free and grafted chains was 90/10 (in weight). This ratio could be decreased by decreasing the quantity of monomer in the initial solution. We rather kept the experimental condition to obtain both, free chains that will be used as matrix in further solar cell, and grafted particles, in “one pot”. The “free” polymer chains were characterized by gel permeation chromatography (figure SI-19) but their insolubility in THF leaded to an under-estimation of molar masses and dispersity. Rather UV-visible spectrometry was performed to show an increase of the absorption maximum wavelength with increasing the polymerization time. Again maximum conjugation length was obtained for PSBTBT 4 and 6 (Figure 1) [21], with an optical band gap of 1.51 eV and an electronical band gap of 1.58 eV (determined by cyclic voltammetry, see SI21-23). ^{1}H and ^{13}C NMR showed all the characteristic peaks of the polymers (figure SI24-26)

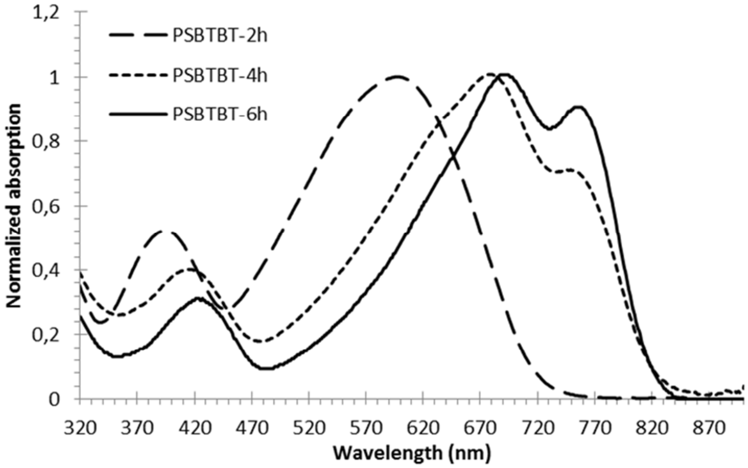

Figure 1. UV-visible absorption spectra in chloroform of free PSBTBT obtained after 2, 4 and 6h of reaction.

At the end of the washing procedure the particles were dark blue/green. XPS characterization was also performed and proved the presence of polymer at the surface with an increase of the carbon and silicon atom contents and a decrease of zinc and oxygen. Moreover there was an appearance of three new elements namely sulfur, silicon (Si-C) and nitrogen pertaining to the monomer unit and in a quantity which increased with polymerization time. Interestingly, the presence of bromine, palladium and tin indicate the presence of active chains indicating the possibility to extend the length of the polymer brush.

Another indication of successful grafting was brought by the silicon binding energy which was divided in two populations: at 102.3 eV for Si-O (the silane anchoring group) and at 100.7 eV for Si-C (the monomer unity). Deconvolution of the Si signal at 103-101 eV showed an increase in the ratio Si-C/Si-O signals area (see figure SI12) with polymerization time. This is also consistent with TGA analysis of the grafted particles revealing an increase in the weight loss percentage with polymerization time (last column Table 1, figure SI13).

Table 1. Chemical composition of the surfaces determined by XPS.

Substrate/Atom	C	O	Zn	Br	Si-O	Si-C	Pd	S	Sn	N	w. l.
Binding energy (eV)	285	530.5	1022.5	70.1	102.8	101.1	335.4	164	487.4	399.4	% [a]
ZnO	19.4	45.6	35.0	-	-	-	-	-	-	-	2.7
ZnO@PhBr	20.3	46.3	28.3	1.5	3.7	-	-	-	-	-	4.1
ZnO@PhPdBr	22.6	43.9	28.4	1.3	2.2	-	1.6	-	-	-	-
ZnO@PSBTBT 2	30.9	37.2	23.1	1.7	2.8	0.5	1	1.1	0.7	1.2	6.3
ZnO@PSBTBT 4	49.1	26.4	12.9	2.2	1.2	1	1	3.12	1.2	2.1	7.4
ZnO@PSBTBT 6	57	21.2	9.4	0.8	1.7	1.6	0.7	4.6	0.7	2.9	13.3

[a] w.l.: weight loss percentage determined by thermogravimetric analysis.

Transmission electronic microscopy (TEM) was used to highlight the thickness of the grafted LBG layer onto the ZnO NRs surface. Figure 2 shows both bare particles and ZnO@PSBTBT 2. A clear, complete and homogeneous polymer shell was identified around ZnO NRs after grafting, leading to core@shell hybrid material. The average polymer shell thickness (h) as measured from the images for the different hybrid nanorods was 5 ± 1 nm.

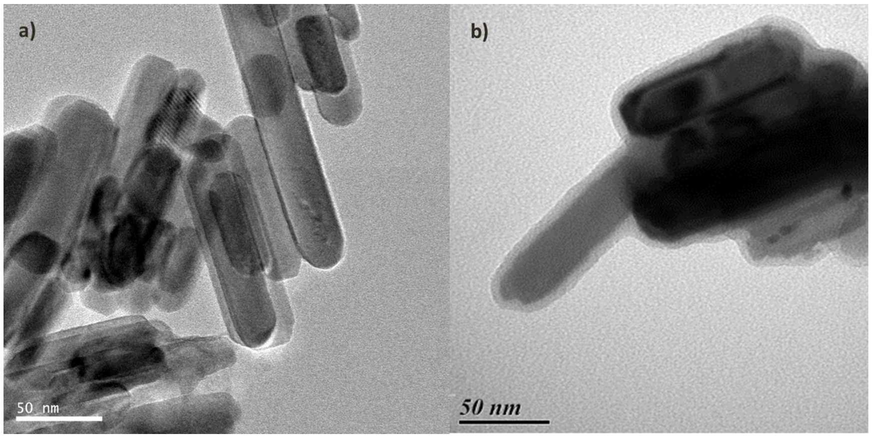

Figure 2. Images recorded by TEM of (a) bare ZnO nanorods and (b) ZnO@PSBTBT 2 (scale bar 50 nm).

TEM analysis of ZnO@PSBTBT 4 and 6 also emphasized this homogeneous layer (see SI15-17) but no clear increase in the shell thickness was detected. Our hypothesis is that this can be explained considering the mechanism of a surface initiated step growth polymerization. During the reaction, monomers and multimers in solution can couple with the surface. If long multimers anchor the surface then a steric hindrance is created, some short surface chains are hidden and their propagation is then limited. This phenomenon is exacerbated with polymerization time since the steric hindrance of the chains grows. Therefore, the ability for long chains to reach active sites at the surface decreases and the grafted chains dispersity increases. As a final consequence the long anchored macromolecules have space to fold over the surface, reducing the apparent thickness of the organic shell. A limitation in this methodology can be demonstrated in figure SI18 in which crosslinking of the nanoparticles by the polymer happened as the conversion or the particle/monomer concentration was too high.

It is interesting to observe that the photophysical properties of the LGB polymer brushes can significantly differ from those of the same polymer in solution. Figure 3 presents the superposition of UV-visible absorbance spectra in chloroform of the grafted ZnO@PSBTBT 2 nanorods, a mixture of bare ZnO nanoparticles/free polymer 2 and finally the free polymer 2 for comparison. The first feature is the presence in the UV region at 370 nm of the ZnO absorption band. Free polymer chains exhibit a maximum absorption at a wavelength of 600 nm which was the same in the case of the mixture, indicating that macromolecules were well solvated in $CHCl_3$ and behaved independently. On the contrary, upon grafting, the maximum absorbance was drastically red-shifted to a wavelength of 680 nm with a clear shoulder at 750 nm.

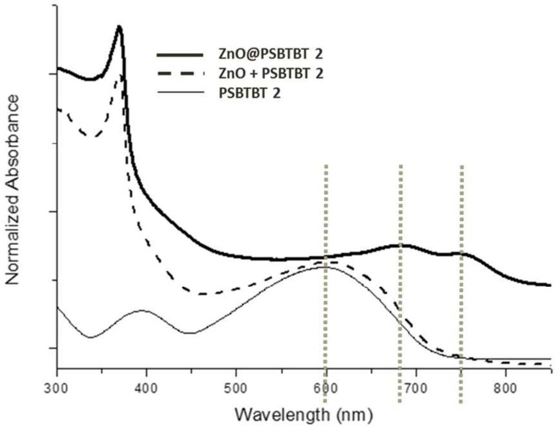

Figure 3. UV-visible spectra of the ZnO@PSBTBT 2 (bold line), ZnO + PSBTBT 2 (dash) and PSBTBT 2 (line) in chloroform solution.

This bathochromic shift, i.e. red shift of 70-80 nm, reflects nicely a significant planarization of the polymer backbone and high inter-chain interaction resulting in efficient delocalization of the π-conjugated electrons. This behaviour is related to the high grafting density of the polymer brushes which forces the macromolecules to be in close contact and packed. Kiriy *et al*. have already observed the same effect for P3HT brushes created on silica particles via the "grafting from" methodology.[10] On the contrary, when the grafting density is lower, like in the case of the "grafting onto" methodology, the anchored polymer is swollen and its maximum absorption remains the same as the corresponding free polymer.[22, 23] As a comparison, thin films of the free polymer were obtained by spin-coating, annealed and their UV-visible spectra presented the same feature that the polymer brushes (Figure SI10). The UV-visible absorbance was also recorded for ZnO@PSBTBT 4 and 6 and showed a high degree of order and packing in the polymer brushes, with a strong increase of the intensity of the vibronic structures peak at 780-800 nm (Figure SI9).

To conclude, the covalent attachment of low band-gap conjugated polymer on an inorganic metal oxide substrate was for the first time demonstrated. Stille polycondensation was successfully initiated from the surface of palladium catalyst-immobilized zinc oxide nanorods. Due to the inherent step growth mechanism of the polymerization, the synthesized polymer was both grafted onto ZnO surfaces and obtained as free macromolecules. XPS and TEM analysis demonstrated that the macromolecules anchored on the nanorods formed a homogeneous organic shell of 5 nm thick. UV-visible spectroscopy exhibited a strong bathochromic effect of 70-80 nm and relevant vibronic structures because of the high grafting density and strong π-π stacking which tend to closely pack the confined polymer chains grafted at the surface. This hybrid

ZnO@LBG, as acceptor@donor material, is the first step toward our target to obtain "patchy" particles with a ZnO core partially covered with low band gap polymer in order to maintain electron percolation between particles.

ASSOCIATED CONTENT

Experimental procedures and additional Figures such as TEM images, thermogravimetric analysis and UV spectra are supplied in Supporting Information. This material is available free of charge via the Internet at http://pubs.acs.org.

AUTHOR INFORMATION

Corresponding Author

laurent.billon@univ-pau.fr, christine.dagron-lartigau@univ-pau.fr

ACKNOWLEDGMENT

This work was supported by the French Ministry of Research and COST Action MP1202 "Rational design of hybrid organic-inorganic interfaces: the next step towards advanced functional materials". The authors thank Dr D. Flahaut for XPS analyses and Dr M.H. Delville for providing ZnO nanoparticles.

REFERENCES

1. A. G. MacDiarmid, *Angewandte Chemie - International Edition*, 2001, **40**, 2581-2590.

2. E. Bundgaard and F. C. Krebs, *Sol. Energy Mater. Sol. Cells*, 2007, **91**, 954-985.
3. A. Pron, P. Berrouard and M. Leclerc, *Macromol. Chem. Phys.*, 2013, **214**, 7-16.
4. X. Guo, N. Zhou, S. J. Lou, J. Smith, D. B. Tice, J. W. Hennek, R. P. Ortiz, J. T. L. Navarrete, S. Li, J. Strzalka, L. X. Chen, R. P. H. Chang, A. Facchetti and T. J. Marks, *Nat. Photonics*, 2013, **7**, 825-833.
5. Z. He, C. Zhong, S. Su, M. Xu, H. Wu and Y. Cao, *Nat. Photonics*, 2012, **6**, 591-595.
6. Y. Liu, J. Zhao, Z. Li, C. Mu, W. Ma, H. Hu, K. Jiang, H. Lin, H. Ade and H. Yan, *Nat Commun*, 2014, **5**.
7. A. Bousquet, H. Awada, R. C. Hiorns, C. Dagron-Lartigau and L. Billon, *Prog. Polym. Sci.*, 2014, **39**, 1847-1877.
8. L. Yang, S. K. Sontag, T. W. Lajoie, W. Li, N. E. Huddleston, J. Locklin and W. You, *ACS Appl. Mater. Interfaces*, 2012, **4**, 5069-5073.
9. S. K. Sontag, N. Marshall and J. Locklin, *Chem. Commun. (Cambridge, U. K.)*, 2009, 3354-3356.
10. V. Senkovskyy, R. Tkachov, T. Beryozkina, H. Komber, U. Oertel, M. Horecha, V. Bocharova, M. Stamm, S. A. Gevorgyan, F. C. Krebs and A. Kiriy, *J. Am. Chem. Soc.*, 2009, **131**, 16445-16453.
11. V. Senkovskyy, N. Khanduyeva, H. Komber, U. Oertel, M. Stamm, D. Kuckling and A. Kiriy, *J. Am. Chem. Soc.*, 2007, **129**, 6626-6632.
12. N. Doubina, J. L. Jenkins, S. A. Paniagua, K. A. Mazzio, G. A. MacDonald, A. K. Y. Jen, N. R. Armstrong, S. R. Marder and C. K. Luscombe, *Langmuir*, 2012, **28**, 1900-1908.
13. S. Kang, R. J. Ono and C. W. Bielawski, *J. Am. Chem. Soc.*, 2013, **135**, 4984-4987.
14. S. B. Jhaveri, J. J. Peterson and K. R. Carter, *Langmuir*, 2009, **25**, 9552-9556.
15. H. Skaff, K. Sill and T. Emrick, *J. Am. Chem. Soc.*, 2004, **126**, 11322-11325.
16. J. Hou, H. Y. Chen, S. Zhang, G. Li and Y. Yang, *J. Am. Chem. Soc.*, 2008, **130**, 16144-16145.
17. W. J. E. Beek, M. M. Wienk and R. A. J. Janssen, *Adv. Funct. Mater.*, 2006, **16**, 1112-1116.
18. L. Whittaker-Brooks, W. E. McClain, J. Schwartz and Y. L. Loo, *Advanced Energy Materials*, 2014, **4**.
19. C. Leow, T. Ohnishi and M. Matsumura, *RSC Advances*, 2015, **5**, 6232-6237.
20. S. K. Sontag, G. R. Sheppard, N. M. Usselman, N. Marshall and J. Locklin, *Langmuir*, 2011, **27**, 12033-12041.
21. M. C. Scharber, M. Koppe, J. Gao, F. Cordella, M. A. Loi, P. Denk, M. Morana, H. J. Egelhaaf, K. Forberich, G. Dennler, R. Gaudiana, D. Waller, Z. Zhu, X. Shi and C. J. Brabec, *Adv. Mater. (Weinheim, Ger.)*, 2010, **22**, 367-370.
22. H. Awada, H. Medlej, S. Blanc, M. H. Delville, R. C. Hiorns, A. Bousquet, C. Dagron-Lartigau and L. Billon, *J. Polym. Sci., Part A: Polym. Chem.*, 2014, **52**, 30-38.
23. J. Xu, J. Wang, M. Mitchell, P. Mukherjee, M. Jeffries-El, J. W. Petrich and Z. Lin, *J. Am. Chem. Soc.*, 2007, **129**, 12828-12833.

Insert Table of Contents Graphic and Synopsis Here

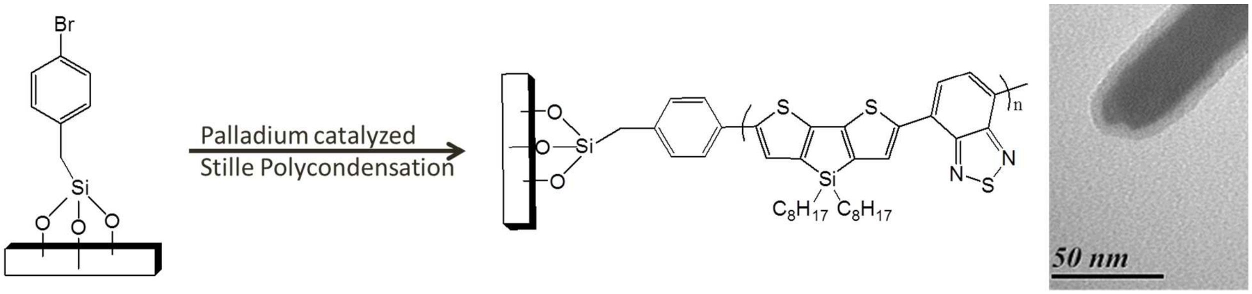

A surface initiated polycondensation that enables access to well-defined core-shell nanoparticles is described. Stille polymerization was initiated from the surface of palladium catalyst-immobilized zinc oxide nanorods. For the first time, a low band gap polymer poly[(4,4’-bis(2-ethylhexyl)dithieno-[3,2-b:2’,3’-d]silole)-2,6-diyl-alt-(2,1,3-benzothiadiazole)-4,7-diyl] (PSBTBT) was anchored on zinc oxide nanorods to elaborate hybrid materials with tunable photophysical properties.